Contributions of the atmosphere-land and ocean-sea ice model components to the tropical Atlantic SST bias in CESM1

Zhenya Song[1,2,3], Sang-Ki Lee[1,2], Chunzai Wang[2], Ben Kirtman[4] and Fangli Qiao[3]

[1]Cooperative Institute for Marine and Atmospheric Studies, University of Miami, Miami FL

[2]Atlantic Oceanographic and Meteorological Laboratory, NOAA, Miami FL

[3]First Institute of Oceanography, State Oceanic Administration, Qingdao China

[4]Rosenstiel School of Marine and Atmospheric Sciences, University of Miami, Miami, Florida

Submitted to Climate Dynamics (1st revision)

August 2014

Corresponding author address: Dr. Sang-Ki Lee, CIMAS, University of Miami, 4600 Rickenbacker Causeway, Miami, FL 33149, USA. E-mail: Sang-Ki.Lee@noaa.gov.

Abstract

In order to identify and quantify intrinsic errors in the atmosphere-land and ocean-sea ice model components of the Community Earth System Model version 1 (CESM1) and their contributions to the tropical Atlantic sea surface temperature (SST) bias in CESM1, we propose a new method of diagnosis and apply it to a set of CESM1 simulations. Our analysis of the model simulations indicates that both the atmosphere-land and ocean-sea ice model components of CESM1 contain large errors in the tropical Atlantic. When the two model components are fully coupled, the intrinsic errors in the two components emerge quickly within a year with strong seasonality in their growth rates. In particular, the ocean-sea ice model contributes significantly in forcing the eastern equatorial Atlantic warm SST bias in early boreal summer. Further analysis shows that the upper thermocline water underneath the eastern equatorial Atlantic surface mixed layer is too warm in a stand-alone ocean-sea ice simulation of CESM1 forced with observed surface flux fields, suggesting that the mixed layer cooling associated with the entrainment of upper thermocline water is too weak in early boreal summer. Therefore, while we acknowledge the potential importance of the westerly wind bias in the western equatorial Atlantic and the low-level stratus cloud bias in the southeastern tropical Atlantic, both of which originate from the atmosphere-land model, we emphasize here that solving those problems in the atmosphere-land model alone does not resolve the equatorial Atlantic warm bias in CESM1.

1. Introduction

Since the pioneering work of Manabe and Bryan (1969), coupled atmosphere-ocean general circulation models (AOGCMs) have significantly improved. AOGCMs are now able to reproduce the basic features of the global climate system (Covey et al. 2003; Meehl et al. 2005), and thus become an important tool for seasonal forecasts, climate projections and other climate research in general.

However, the tropical Atlantic biases typically characterized by warmer sea surface temperatures (SSTs) in the eastern equatorial ocean, a reversed zonal SST gradient along the equator, colder SSTs in the northwest and southwest tropical Atlantic, and warmer SSTs in the northeast and southeast tropical Atlantic, are common problems with most AOGCMs (e.g., Davey et al. 2002).

Model biases have been somewhat reduced in most recent models used in the Coupled Model Intercomparison Project Phase 5 (CMIP5) compared to those used in CMIP3 (e.g., Liu et al. 2013). Recent studies have also shown that improving the spatial resolution could potentially reduce such biases (Gent et al. 2010; Patricola et al. 2011; Kirtman et al. 2012). Nevertheless, almost all of the state-of-the-art AOGCMs still cannot reproduce the climatology of tropical Atlantic SSTs (Mechoso et al. 1995; Davey et al. 2002; Covey et al. 2003; Huang et al. 2007; Richter and Xie 2008; Richter et al. 2012).

These systematic tropical Atlantic biases in AOGCMs will affect the models' ability to simulate and predict climate variability (Xie and Carton 2004). Studies have shown that the tropical Atlantic affects and modulates climate variability of the Western Hemisphere, such as the West African summer monsoon (Vizy and Cook 2001; Giannini et al. 2003; Gu and Adler 2004), moisture transport and rainfall over the American continents (Enfield et al. 2001; Wang et al. 2006) and Atlantic hurricane development and intensification (e.g., Goldenberg et al. 2001; Webster et al. 2005; Wang and Lee 2007). Therefore, in order to increase the seasonal-to-decadal climate predictability in the Western Hemisphere, it is important to accurately simulate the tropical Atlantic Ocean in AOGCMs. It is also worthwhile to point out that the tropical Atlantic problem in AOGCMs is one of the most critical obstacles for achieving confidence in our model-based future projection of the global SST warming patterns (e.g., Xie et al. 2010; Lee et al. 2011; DiNezio et al. 2012).

Many studies have diagnosed the large systematic errors in the tropical Atlantic, and attributed the errors to various atmospheric and/or ocean processes. Recent studies argued that the westerly wind bias over the western tropical Atlantic in boreal spring is the main cause of the tropical Atlantic biases (Richter and Xie 2008; Richter et al. 2012), and showed that the westerly wind bias also exists in the atmosphere general circulation models (AGCMs) forced by observed SSTs (DeWitt 2005; Chang et al. 2007; Richter and Xie 2008; Richter et al. 2012). These studies argued that the westerly wind bias in boreal spring deepens the thermocline in the eastern equatorial Atlantic and prevents the development of the cold tongue in boreal summer; then warm SST bias develops in the cold tongue and further amplifies due to the Bjerknes feedback.

Other studies have suggested that a likely source of the tropical Atlantic biases is the deficiency of AOGCMs in reproducing the low-level stratus cloud deck over the southeastern tropical Atlantic Ocean (Yu and Mechoso 1999; Large and Danabasoglu 2006; Saha et al. 2006; Huang et al. 2007; Hu et al. 2008; 2011; Richter and Xie 2008). These studies argue that the warm SST bias over the southeastern tropical Atlantic is mainly caused by the model's inability to reproduce the observed amount of low-level cloud in the region, which in turn causes an excessive local shortwave radiative flux into the ocean. Wahl et al. (2011) explored this hypothesis by performing some sensitivity experiments using the Kiel Climate model. Wahl et al. (2011) concluded that the westerly wind bias over the western tropical Atlantic in spring and early summer is the key mechanism for the equatorial Atlantic SST bias, while the low-level cloud cover and associated excessive surface shortwave radiation contribute to the SST bias in the southeast tropical Atlantic Ocean.

There are also some studies suggesting that ocean processes could contribute to the tropical Atlantic biases. Hazeleger and Haarsma (2005), for example, suggested that the tropical Atlantic bias is strongly related to the upper ocean mixing. Seo et al. (2006) argued that properly representing equatorial Atlantic instability waves in climate models could enhance the equatorial upwelling and thus potentially reduce the equatorial Atlantic warm SST bias. Large and Danabasoglu (2006) suggested that the warm SST bias in the southeastern tropical Atlantic could be reduced by improving the simulation of coastal upwelling off the coasts of southwest Africa. Xu et al. (2014) stressed that the inability of AOGCMs in simulating the Angola–Benguela front is one the leading causes of the tropical Atlantic SST biases. Breugem et al. (2008) attributed the warm SST bias in the eastern and southeastern tropical Atlantic to the spurious barrier layer (BL), which forms due to the excessive regional rainfall and amplifies via coupled SST-precipitation-BL feedback and thus prevents surface cooling via strong salinity stratification. However, Richter et al. (2012) showed that the BL feedback described by Breugem et al. (2008) is not significant at least in the Geophysical Fluid Dynamics Laboratory (GFDL) coupled model. There are also other interesting hypotheses on the origin of the tropical Atlantic SST bias in the coupled models, such as the remote influence from higher latitudes (Lee and Wang 2008; Chang et al. 2007), the West African monsoon (Deser et al. 2006), rainfall over the Amazon and Africa

(Davey et al. 2002; Chang et al. 2008; Okumura and Xie 2004), and air-sea turbulent flux (Ban et al. 2010).

Previous studies such as those briefly reviewed above have suggested a variety of potential causes of the tropical Atlantic SST biases in AOGCMs. However, these hypotheses (or conclusions) are derived mostly based on fully spun up AOGCM runs. Since the SST bias in an AOGCM could cause errors in the atmospheric circulation, which in turn also could feedback onto the tropical Atlantic SSTs via air-sea interaction, it is almost impossible to identify the exact processes responsible for the tropical Atlantic SST bias from fully spun up AOGCM runs. It is also worthwhile to note that a quantitative analysis on the contributions of the atmosphere-land model and ocean-sea ice model components to the tropical Atlantic SST bias in an AOGCM has rarely been done. Therefore, in an effort to better understand what causes the tropical Atlantic SST biases, here we propose a new methodology to analyze the SST bias focusing on the initial development of the SST bias by using the National Center for Atmospheric Research (NCAR) Community Earth System Model version 1 (CESM1), which suffers the same systematic tropical Atlantic SST bias as in other AOGCMs.

This paper is organized as follows. The model and numerical experiments design are described in section 2. The experiment results and analysis are presented in section 3 ~ 6, in which the SST bias and its development mechanism in CESM1 are analyzed by comparing results from three model experiments (to be described in section 2). Section 7 provides conclusions and discussion.

2. Model and model experiments

CESM1 is a state-of-the-art global earth system model that can provide simulations of the Earth's past, present, and future climate. It is the successor to the Community Climate System Model (CCSM), which was extended and renamed to CESM in June 2010. CESM1, which was released in November 2012, is a superset of CCSM4 in that its default configuration is the same science scenarios as CCSM4, although CESM1 also contains options for a terrestrial carbon cycle and dynamics, and ocean ecosystems and biogeochemical coupling, all necessary for an earth system model. In this paper, CESM1 is configured as a purely physical model, and is thus identical to CCSM4, since our focus here is on the physical processes.

Many improvements have been made in CESM1/CCSM4 simulations compared with the previous version of CCSM3, such as the frequency of the Madden - Julian Oscillation (MJO) and ENSO variability, the annual cycle of SSTs in the eastern equatorial Pacific, and the Arctic sea-ice concentration (Gent et al. 2011). However, it still displays significant tropical Atlantic SST biases (Grodsky et al. 2012) as shown in Figure 1c. The observed SSTs in the equatorial Atlantic are warmer in the west and cooler in the east (Figure 1a). However, the SSTs in the CCSM4 control simulation with twentieth century forcing (CCSM4_20C hereafter), which is available from the CMIP5 archive, are warmer in the east and cooler in the west with the SST bias exceeding 3.0°C in the southeast tropical Atlantic along the east coast of Africa (Figure 1b). It is clear that CCSM4_20C fails to reproduce the equatorial Atlantic cold tongue and the zonal SST gradient along the equator, which are common deficiencies in AOGCMs.

The main objective of this study is to identify the processes responsible for the development of the tropical Atlantic SST biases in CESM1. Our approach to achieve this goal is to diagnose the development of biases in a fully coupled CESM1 run initialized with data from uncoupled surface-forced atmosphere and ocean only simulations. This approach is analogous to the methodology proposed in the Transpose-Atmospheric Model Intercomparison Project Phase II (T-AMIP2) as discussed in Williams et al. (2013). Similar methods were also used in previous studies (e.g., Huang et al. 2007; Toniazzo and Woolnough 2013; Voldoire et al. 2014).

Three numerical experiments are designed and performed using CESM1. These experiments are (1) dynamic atmosphere-land run forced by observed SSTs (EXP_ATM hereafter); (2) dynamic ocean-sea ice run forced by observed surface atmospheric fluxes (EXP_OCN hereafter); and (3) fully coupled atmosphere-land-ocean-sea ice run initialized with data from EXP_ATM and EXP_OCN (EXP_CPL hereafter).

The atmosphere model component is Community Atmosphere Model version 4 (CAM4; Neale et al. 2010) and the land model is Community Land Model version 4 (CLM4; Lawrence et al. 2011). Both CAM4 and CLM4 have horizontal resolution of 1.9° × 2.5°, and are forced by observed climatological monthly SSTs (Hurrell et al. 2008). This experiment (EXP_ATM) is integrated for 30 years and the last ten years are used for analysis. The ocean model is Parallel Ocean Program version 2 (POP2; Danabasoglu et al. 2012) and the sea-ice model is Community Ice Model version 4 (CICE4; Hunke and Lipscomb 2008). Both POP2 and CICE4 have a nominal 1° horizontal resolution, and are forced by Coordinated Ocean Reference Experiment phase 2 (COREv2) normal-year surface fluxes (Large and Yeager 2004; 2009). This experiment (EXP_OCN) is integrated for 210 years and the last ten years are used for analysis.

For the fully coupled experiment (EXP_CPL), 10-member ensemble experiments are performed to achieve statistically significant model results. The atmosphere and surface land models are initialized using EXP_ATM while the ocean and sea-ice models are initialized using EXP_OCN. The 10-member ensemble experiments are initialized using the combination of the EXP_ATM and EXP_OCN obtained from the last 10 years of the model integrations, and integrated for five years. In the following sections, the ensemble-mean of EXP_CPL along with the results from EXP_ATM and EXP_OCN are analyzed to identify the processes that cause the development of the tropical Atlantic SST biases in CESM1.

3. Implicit SST bias in EXP_ATM and EXP_OCN

3.1 EXP_ATM

In order to understand and quantify the roles of the atmospheric-land model (EXP_ATM) in the generation of the tropical Atlantic SST bias, the net surface heat flux bias in EXP_ATM is integrated in time:

$$\Delta T_{\mathrm{EXP\_ATM}}(t) = \int_0^t \frac{Q_{NET}[\mathrm{EXP\_ATM}] - Q_{NET}[\mathrm{OBS}]}{\rho_w C_{pw} D} dt, \quad (1)$$

where ρ_w is sea water density, C_{pw} is the specific heat of sea water, D is the mixed layer depth from EXP_OCN, Q_{NET}[EXP_ATM] and Q_{NET}[OBS] are the net surface heat fluxes from EXP_ATM and COREv2, respectively. Note that $\Delta T_{\mathrm{EXP\_ATM}}$ represents SST bias, which could be potentially caused by the net surface heat flux bias for the duration of t, with assumptions that the atmosphere-land model is coupled with a perfect ocean (i.e., all oceanic heat flux terms are error-free) and there is no air-sea feedback to amplify or damp out the net surface heat flux bias. Obviously, the net heat flux bias in this case (EXP_ATM) does not change the model SSTs because the model SSTs are fixed. Therefore, it is referred to as *implicit SST bias* in EXP_ATM, hereafter.

Figure 2a shows the annually averaged implicit SST bias in EXP_ATM due to the net surface heat flux bias. This is computed by integrating the long-term averaged net heat flux bias in EXP_ATM from January 1 to December 31, then dividing it by 12 months. Using a similar method, the annually averaged implicit SST bias in EXP_ATM due to the latent heat flux, shortwave radiative heat flux, and longwave radiative heat flux, are computed and shown in Fig. 2b, c, and d, respectively. As shown in Fig. 2a, the north-central equatorial Atlantic and also the southeastern tropical Atlantic between 20°S and the equator are characterized by warm (implicit) SST bias; while in other regions, especially in the south and north tropical Atlantic, there are two bands of cold (implicit) SST bias across the Atlantic basin. These results suggest that if the atmosphere-land model is coupled with a perfect ocean and the SST bias does not feedback onto the atmosphere-land model, warm SST bias is expected in the north-central equatorial Atlantic and the southeastern tropical Atlantic, whereas cold SST bias is expected in the north and south tropical Atlantic.

Figure 2c shows that the warm/cold implicit SST biases in EXP_ATM are mainly caused by weaker/stronger surface wind stress bias and associated positive (i.e., into the ocean)/negative (i.e., out of the ocean) latent heat flux bias. As shown in Fig. 2b, the shortwave radiative flux is larger than observations over the stratus cloud deck region of the south-central and southeastern tropical Atlantic Ocean, south of around 10°S (Large and Danabasoglu 2006; Huang et al. 2007; Grodsky et al. 2012). Although not shown here, CCSM4_20C also contains the positive shortwave radiative flux bias in the southeastern tropical Atlantic with about the same amplitude of that in EXP_ATM, suggesting that the low-level cloud and shortwave radiation errors in CCSM4_20C are inherent to its atmospheric-land component.

3.2 EXP_OCN

Figure 3 shows the SST bias in the surface-forced ocean-sea ice model experiment (EXP_OCN). Overall, the tropical Atlantic SSTs are reasonably well simulated with a relatively low amplitude of SST bias. Nevertheless, the amplitude of warm SST bias in the southeastern tropical Atlantic especially near the west coast of Africa is quite large (up to 2°C). This suggests that inherent errors in the ocean-sea ice model can significantly contribute to the warm SST bias in CCSM4_20C, in agreement with earlier studies (Large and Danabasoglu 2006; Grodsky et al. 2012).

It is important to note that in EXP_OCN the ocean-sea ice model is forced with prescribed atmospheric conditions. Flux forms of atmospheric forcing, namely short and longwave radiative heat fluxes, precipitation rate and wind stress are directly used to force the ocean-sea ice model. For latent and sensible heat fluxes, however, bulk equations are used to compute them interactively using wind speed, air humidity and air temperature at 10 m along with the model SSTs. Such a treatment of the turbulent heat fluxes ultimately relaxes the model SSTs toward the prescribed surface air temperature as discussed in earlier studies (e.g., Lee et al. 2007; Liu et al. 2012). Therefore, the SST bias in EXP_OCN shown in Fig. 3 is not a good measure of inherent errors in the ocean-sea ice model.

To better quantify the inherent errors in EXP_OCN, we attempt to compute implicit SST bias in EXP_OCN associated with spurious ocean dynamic processes. The equation for the surface mixed layer temperature bias in EXP_OCN can be written as

$$\frac{\partial \Delta T_m}{\partial t} = -\Delta\left(u_m \frac{\partial T_m}{\partial x} + v_m \frac{\partial T_m}{\partial y} + w_e \left(T_m - T_e \right) \right) + \frac{Q_{NET}\left[\text{EXP\_OCN}\right] - Q_{NET}\left[\text{OBS}\right]}{\rho_w C_{pw} D}, \qquad (2)$$

where ΔT_m is the difference in ocean mixed layer temperature between EXP_OCN and the observation, u_m and v_m are the ocean mixed layer currents in the x- and y-directions, w_e is the entrainment rate at the mixed layer base, T_e is the ocean temperature immediately below the mixed layer, and Q_{NET} [EXP_OCN] is the net surface heat flux in EXP_OCN (see Lee et al. 2007 for the derivation of the bulk mixed layer temperature equation). The first three terms on the right side of equation (2) can be regarded as the errors in ocean dynamic processes. Integrating equation (2) in time, after a minor manipulation, we get

$$\Delta T_{\text{EXP\_OCN}} \equiv -\int_0^t \Delta\left(u_m \frac{\partial T_m}{\partial x} + v_m \frac{\partial T_m}{\partial y} + w_e\left(T_m - T_e\right)\right) dt \\ = \Delta T_m - \int_0^t \frac{Q_{NET}\left[\text{EXP\_OCN}\right] - Q_{NET}\left[\text{OBS}\right]}{\rho_w C_{pw} D} dt. \tag{3}$$

$\Delta T_{\text{EXP\_OCN}}$ represents the implicit SST bias in EXP_OCN due to the inherent errors in the ocean dynamic processes, including advection and turbulent mixing, for the duration of *t* with assumptions that there is no air-sea feedback to amplify or damp out the net surface heat flux bias.

Figure 4a shows the annually averaged implicit SST bias in EXP_OCN linked to spurious ocean dynamic processes. Its amplitude is of the same order of magnitude as that in EXP_ATM (Fig. 2a). Comparing Fig. 4a with Fig. 2a, in the southeastern and northeastern tropical Atlantic, especially near the west coast of Africa, the implicit SST bias due to spurious ocean dynamic processes is much larger than that due to net heat flux bias in EXP_ATM. This strongly suggests that the warm SST biases in CCSM4_20C over these regions (see Fig. 1b) are mainly associated with spurious ocean dynamic processes.

It is interesting to note that ocean dynamic cooling in EXP_OCN is too strong in the eastern equatorial Atlantic, but too weak in the central equatorial Atlantic. Given that vertical entrainment of cold thermocline water due to turbulent mixing is what maintains the cold tongue in the central equatorial Atlantic (e.g., Lee and Csanady 1999a; 1999b; Goes and Wainer 2003), it is possible that the parameterization of vertical mixing, and/or the mean state variables that affect the vertical mixing, namely vertical shear and stratification at the mixed layer base, are the source of the SST bias. It is also possible that failing to resolve equatorial Atlantic instability waves reduces the equatorial upwelling and is thus responsible for the warm implicit SST bias in the central equatorial Atlantic (Seo et al. 2006).

3.3 EXP_ATM + EXP_OCN

The linear combination of the implicit SST bias in EXP_ATM due to net surface heat flux bias (1) and the implicit SST bias in EXP_OCN due to spurious ocean dynamic processes (3) can be written as

$$\Delta T_{\mathrm{EXP\_ATM}} + \Delta T_{\mathrm{EXP\_OCN}} = \Delta T_m + \int_0^t \frac{Q_{NET}\left[\mathrm{EXP\_ATM}\right] - Q_{NET}\left[\mathrm{EXP\_OCN}\right]}{\rho_w C_{pw} D} dt. \tag{4}$$

This total implicit SST bias is directly linked to the net surface heat flux mismatch between EXP_ATM and EXP_OCN, and is what is expected when the atmosphere-land model is joined together with the ocean-sea ice model but without any air-sea feedback. It is important to note that the implicit SST bias in EXP_ATM + EXP_OCN is independent from the observed surface heat flux product used in the analysis, and is thus not subject to uncertainty in the observed (or referenced) surface heat flux product used at least in a linear sense.

Figure 4b shows the total implicit SST bias in EXP_ATM + EXP_OCN. Comparing this with the SST bias in CCSM4_20C (Fig. 1b), their spatial patterns are surprisingly similar. In particular, in both CCSM4_20C and EXP_ATM + EXP_OCN, the southwestern and northwestern tropical Atlantic are characterized by cold SST bias, while the southeastern and northeastern tropical Atlantic are characterized by warm SST bias. This result mainly suggests that the cold/warm SST biases over these off-equatorial regions in CCSM4_20C originate from the intrinsic biases in the atmosphere-land and ocean-sea ice model components, and further weakened/amplified by atmosphere-ocean coupling.

It is noted that the overall amplitude of the SST bias in CCSM4_20C is smaller than the amplitude of the total implicit SST bias in EXP_ATM + EXP_OCN. This is not unexpected because the total implicit bias in EXP_ATM + EXP_OCN estimates the extent to which the spurious atmosphere-ocean dynamics in the atmosphere-land and ocean sea-ice model components could *potentially* contribute to the SST bias once the air-sea coupling is initiated. For instance, in a region where the total implicit SST bias is positive, once the air-sea coupling is initiated, the model SSTs will increase initially. However, the increased SSTs will in turn enhance the longwave radiative and latent cooling at the surface to reduce the rate of SST warming. Therefore, it is highly unlikely that the SST bias will reach the full extent of the total implicit SST bias.

It is interesting to note that the implicit SST bias in EXP_OCN (Fig. 4b) is slightly negative over the eastern equatorial Atlantic region. This is somewhat inconsistent with the SST bias in CCSM4_20C over the same region (Fig. 1b). Therefore, to better understand the origin of the equatorial Atlantic SST bias in CCSM4_20C, in the next section we explore the initial development of the tropical Atlantic SST bias in EXP_CPL. It is shown in the next section that the ocean-sea ice model does contribute significantly in forcing the eastern equatorial Atlantic warm SST bias due to its spurious ocean dynamic processes. However, its influence is limited only in early boreal summer during which massive entrainment of the equatorial cold thermocline water into the surface mixed layer occurs (e.g., Lee and Csanady 1999a; 1999b).

4. Initial development of the SST bias in EXP_CPL

Figure 4c shows the SST bias in EXP_CPL averaged over the first year. Overall, both the amplitude and spatial pattern of the SST bias in EXP_CPL developed over the first year are very similar to those of the annually averaged SST bias in CCSM4_20C (Fig. 1b), suggesting that the tropical Atlantic SST bias develops very quickly (note the different scales used in Fig. 1b and Fig. 4c).

Figure 5 shows the bi-monthly SST bias development in the fully coupled model experiment (EXP_CPL) during the first and second years of the model integration. An interesting point is that the cold SST bias in the eastern equatorial Atlantic, which apparently originates from the ocean-sea ice model (Fig. 4a), persists only during the first four months of the coupled model integration. It disappears afterward and is completely masked by the warm SST bias in June of the first year. Among other features, perhaps the most striking is the fast development of the warm SST bias in the southeastern tropical Atlantic - the SST bias along the coast of Angola exceeds 6°C by June of the first year.

Although the tropical Atlantic SST bias in EXP_CPL develops very quickly within a year, largely due to the combined effect of intrinsic biases in EXP_ATM and EXP_OCN, in some regions the SST bias in the first year is further weakened or amplified, probably due to the active atmosphere-ocean coupling. For instance, the cold SST bias over the southwestern tropical Atlantic in the first year is much reduced in the second year due to the eastward expansion of the warm SST anomalies in the southeastern tropical Atlantic. It is also clear that the warm SST bias in the eastern equatorial Atlantic during the first year strengthens and expands westward in the second year.

In order to better describe the tropical Atlantic SST biases in EXP_CPL and how they are forced by EXP_ATM, EXP_OCN and the atmosphere-ocean coupling, the bi-monthly tropical Atlantic SST bias tendencies (°C month^{-1}) in EXP_CPL, EXP_ATM + EXP_OCN, EXP_ATM and EXP_OCN during the first year are shown in Fig. 6. It is clearly shown that the southeastern tropical Atlantic warm SST bias in EXP_CPL, which is largely forced in boreal spring, is caused by EXP_OCN due to spurious ocean dynamic processes, with an assumption that the surface fluxes prescribed in EXP_OCN is error-free. It is also clear that the initial development of the eastern equatorial warm SST bias, which is mainly forced in early boreal summer, is also caused by EXP_OCN due to spurious ocean dynamic processes. By comparing the SST bias tendency in EXP_CPL and the implicit SST bias tendency in EXP_OCN, it is clear that the atmosphere-ocean coupling tends to weaken the implicit SST bias tendency in these regions. This clearly suggests that the atmosphere-ocean coupling is not the cause of the eastern equatorial warm SST bias at least in the first year of the coupling. These features in the equatorial Atlantic are much more clearly illustrated in Fig. 7, which shows the time evolutions of the SST bias tendencies (implicit SST bias tendencies) along the equatorial Atlantic and the contributions by the surface heat flux errors and by errors involving ocean dynamic processes in EXP_CPL (EXP_ATM and EXP_OCN). Therefore, we may conclude that the eastern equatorial and southeastern tropical Atlantic warm SST biases in EXP_CPL are mainly forced by EXP_OCN due to its spurious ocean dynamic processes during boreal spring and summer.

Richter and Xie (2008) analyzed CMIP3 models and argued that the westerly wind bias in boreal spring over the western equatorial Atlantic deepens the thermocline in the eastern equatorial Atlantic preventing the development of the cold tongue in boreal summer, and thus is the root cause of the equatorial Atlantic warm SST bias in CMIP3 models. Our analysis of the three CESM1 experiments, however, suggests that the ocean-sea ice model due to its spurious ocean dynamic processes may contribute more significantly than the atmosphere-land model to the eastern equatorial Atlantic warm SST bias in CCSM4/CESM1. Therefore, while we acknowledge the potential importance of the westerly wind bias in boreal spring over the western equatorial Atlantic, which originates from the atmosphere-land model (see Fig. 2b), here we stress that solving this problem in the atmosphere-land model alone does not resolve the equatorial Atlantic warm bias in CCSM4/CESM1.

Grodsky et al. (2012) showed that mean sea level pressure in CCSM4 is erroneously high by a few millibars in the subtropical highs and erroneously low in the polar lows similar to CCSM3, and thus the trade winds are 1 ~ 2 m s^{-1} too strong. Since the cold SST biases in the southwestern and northwestern tropical Atlantic are closely linked to the strength of the trade winds in EXP_ATM, it is likely that their root cause is linked to the subtropical highs in the atmosphere-land model.

5. Equatorial Atlantic subsurface temperature bias in EXP_OCN

The methodology used in this study only provides a mean to estimate the integrated effects of the spurious ocean dynamic processes in EXP_OCN via “implicit SST bias”. To further understand what causes the spurious ocean dynamic processes, the equatorial Atlantic subsurface temperature bias in EXP_OCN is explored here. Figure 8 shows the monthly-averaged equatorial Atlantic temperature bias (averaged for 5ºS - 5ºN) in EXP_OCN for the upper 200 m. In order to compute the temperature bias, we use EN4, which is a global quality controlled ocean temperature data set provided by the Met Office Hadley Centre (Good et al. 2013). The green lines show the corresponding mixed layer depths obtained from EXP_OCN (solid line) and EN4 (dashed line).

This figure clearly shows that the temperature bias near the surface is quite small because the model-simulated surface temperature is strongly damped to the prescribed air temperature and specific humidity. However, at the based of the model-simulated mixed layer, the temperature bias increases up to 6^{o}C. This suggests that due to spurious ocean dynamic processes in the ocean-sea ice model, the upper thermocline water entrained into the mixed layer during early summer (e.g., Lee and Csanady 1999a; 1999b) is too warm. Therefore, once the ocean sea-ice model is fully coupled to the atmosphere-land model, the extra heat in the mixed layer caused by the entrainment of the warmer-than-observed upper thermocline layer will produces warm SST bias in the equatorial Atlantic upwelling region.

Figure 8 also shows that the mixed layer depth is too deep in EXP_OCN. This suggests that the vertical turbulent mixing may be too intense in EXP_OCN. It is likely that the warmer-than-observed upper thermocline layer weakens the vertical stratification over the upper thermocline and thus contributes to increase turbulent mixing at the mixed layer base. To further investigate what processes or parameterizations are responsible for the warmer-than-observed upper thermocline, it is necessary to perform sensitivity experiments by using the stand-alone ocean sea-ice model and the diagnostic methodology proposed in this study.

6. Impact of uncertainty in the reference surface flux fields

It should be pointed out that our results are not entirely independent from uncertainty in the reference surface flux product used (i.e., COREv2). For instance, if the net surface heat flux in COREv2 is too large, it will contribute positively (negatively) to the implicit SST bias in EXP_OCN (EXP_ATM) according to equations (1) and (3). Although considerable effort was invested to minimize errors (see Large and Yeager 2008 for more details), COREv2 is still far from error-free. Therefore, in a more strict sense, equation (3) should be considered as the implicit SST bias in EXP_OCN referenced to COREv2. Similarly, equation (1) should be considered as the implicit SST bias in EXP_ATM referenced to COREv2. Nevertheless, it should be noted that the total implicit SST bias in EXP_ATM + EXP_OCN is independent from the reference surface flux product used, and is thus not subject to uncertainty in the reference surface flux product at least in a linear sense (see equation 3).

To better understand if and how the uncertainty in the reference surface flux product influences the implicit SST bias in EXP_ATM and EXP_OCN, two additional experiments are performed by forcing the stand-alone ocean sea-ice model for 120 years with the surface flux fields derived from the European Centre for Medium-Range Weather Forecasts Interim (ERA_INT) reanalysis (Dee et al. 2011), and the Modern-Era Retrospective Analysis for Research and Applications (MERRA) reanalysis (Rienecker et al. 2011)

As shown in Figure 9a, d and g, the implicit SST bias in EXP_ATM referenced to either ERA_INT or MERRA is more negative compared to that referenced to COREv2. On the contrary, the implicit SST bias in EXP_OCN referenced to either ERA_INT or MERRA is more positive compared to that referenced to COREv2. What these mean is that the net surface heat flux into the tropical Atlantic is larger overall in ERA_INT and MERRA than that in COREv2. Nevertheless, the spatial patterns of the implicit SST bias in EXP_ATM referenced to the three surface flux products (i.e., COREv2, ERA_INT and MERRRA) are quite similar. As shown in Figure 9b, e and h, the same conclusion can be drawn for the implicit SST bias in EXP_OCN.

In sum, the overall magnitude of the implicit SST bias can be attributed more to either the atmosphere-land model or the ocean sea-ice model depending on the reference surface flux product used. However, the spatial pattern of the implicit bias in EXP_ATM (EXP_OCN) is largely determined by inherent deficiency of the atmosphere-land (ocean-sea ice) model component. As such, the total implicit SST bias in EXP_ATM + EXP_OCN is only minimally affected by the reference surface flux product used (see Figure 9c, f and i). Therefore, we can conclude that the total implicit bias in EXP_ATM + EXP_OCN is a reliable measure of inherent deficiency in CESM1

7. Summary and Discussions

In order to better understand the initial development of the tropical Atlantic SST bias in AOGCMs, we have performed a series of model experiments using CESM1. These experiments are a forced atmosphere-land model experiment (EXP_ATM), a forced ocean-ice model experiment (EXP_OCN) and a fully coupled model experiment with its atmosphere-land model initialized using EXP_ATM and the ocean-ice model using EXP_OCN (EXP_CPL).

We propose and use a new method of diagnosis to identify and quantify intrinsic errors in the atmosphere-land and ocean-sea ice model components of CESM1. It is shown here that both the atmosphere-land and ocean-sea ice model components contain significant errors in the tropical Atlantic. In boreal summer, the ocean-sea ice model could cause large amplitudes of warm SST bias in the eastern equatorial and southeastern tropical Atlantic due to its spurious ocean dynamic processes even if it is coupled to a perfect atmosphere-land model and the SST bias does not feedback onto the ocean-sea ice model. In the atmosphere-land model, the trade winds and associated surface latent cooling are too strong in the northwestern and southwestern tropical Atlantic, while they are too weak in the northeastern and southeastern tropical Atlantic. Therefore, even if the atmosphere-land model is coupled to a perfect ocean-sea ice model and the SST bias does not feedback onto the atmosphere-land model, warm (cold) SST bias could be generated in the northeastern (northwestern) and southeastern (southwestern) tropical Atlantic.

In the fully coupled model simulation with its atmosphere-land model initialized using EXP_ATM and the ocean-sea ice model using EXP_OCN, the tropical Atlantic SST bias develops very quickly within a year, and its seasonality and spatial pattern are largely determined by the linear combination of the implicit SST bias in EXP_ATM and EXP_OCN. In particular, it is shown here that the eastern equatorial and southeastern tropical Atlantic warm SST bias in the fully coupled simulation are forced in early boreal summer by the ocean-sea ice model due to its spurious ocean dynamic processes. Further analysis shows that the upper thermocline water underneath the eastern equatorial Atlantic surface mixed layer is too warm in EXP_OCN. This suggests that the mixed layer cooling in boreal summer associated with the equatorial entrainment of upper thermocline water is too weak.

The main emphasis in this paper is to explore how the tropical Atlantic SST bias in CESM1 is initiated and evolves. Although we identify that the intrinsic errors in the ocean-sea ice model contribute significantly to the tropical SST bias in CESM1, the potential impact of mixed layer depth bias in EXP_OCN is not explored in this study, and thus should be examined in the future work. It should be pointed out that our results are not entirely independent from uncertainty in the reference surface flux product used. Nevertheless, the total implicit SST bias in EXP_ATM + EXP_OCN is only minimally affected by uncertainty in the reference surface flux product used, and thus is a reliable measure of inherent deficiency in CESM1. Further studies are also needed to trace the parameterizations and/or configurations in the ocean-sea ice model that are directly linked to the errors. Therefore, we recommend sensitivity studies on model resolutions (in both the horizontal and vertical directions), vertical mixing schemes and isopycnal mixing schemes, using the ocean-sea ice model component of CESM1 and the diagnosis method proposed in this study.

Acknowledgments. We would like to thank three anonymous reviewers for their thoughtful comments and suggestions, which led to a significant improvement of the paper. We also would like to thank Marlos Goes and Libby Johns for their helpful comments. This research was supported by National Science Foundation Grant ATM-0850897, the National Natural Science Foundation of China (NSFC) through grant 41476023, International Cooperation Project of Ministry of Science and Technology of China 2011DFA20970, the Public Science and Technology Research Funds Projects of Ocean 201105019, and the base funding of NOAA Atlantic Oceanographic and Meteorological Laboratory (AOML). All model simulations used in this study were carried out at National Supercomputer Center in Tianjin, China, and by using NOAA high performance computing system in Boulder, Colorado.

References

Ban J, Gao Z, Lenschow DH (2010) Climate simulations with a new air-sea turbulent flux parameterization in the National Center for Atmospheric Research Community Atmosphere Model (CAM3). J Geophys Res 115:D01106. doi:10.1029/2009JD012802

Breugem W-P, Chang P, Jang CJ, Mignot J, Hazeleger W (2008) Barrier layers and tropical Atlantic SST biases in coupled GCMs. Tellus A 60:885-897. doi:10.1111/j.1600-0870.2008.00343.x

Chang C-Y, Carton JA, Grodsky SA, Nigam S (2007) Seasonal climate of the tropical Atlantic sector in the NCAR Community Climate System Model 3: error structure and probable causes of errors. J Clim 20: 1053–1070

Chang C-Y, Nigam S, Carton JA (2008) Origin of the springtime westerly bias in equatorial Atlantic surface winds in the Community Atmosphere Model version 3 (CAM3) simulation. J Clim 21:4766-4778

Covey C, AchutaRao KM, Cubasch U, Jones P, Lambert SJ, Mann ME, Phillips TJ, Taylor KE (2003) An overview of results from the Coupled Model Intercomparison Project. Global Planet Change 37:103-133

Danabasoglu G, Bates SC, Briegleb BP, Jayne SR, Jochum M, Large WG, Peacock S, Yeager SG (2012) The CCSM4 Ocean Component. J Clim 25:1361–1389. doi:http://dx.doi.org/10.1175/JCLI-D-11-00091.1

Davey M, and coauthors (2002): STOIC: a study of coupled model climatology and variability in tropical ocean regions. Clim Dyn 18:403-420

Dee DP et al (2011) The ERA-Interim reanalysis: configuration and performance of the data assimilation system. QJR Meteorol Soc 137:553-597. doi:10.1002/qj.828

Deser C, Capotondi A, Saravana R, Phillips AS (2006) Tropical Pacific and Atlantic climate variability in CCSM3. J Clim 19:2451-2481

DeWitt DG (2005) Diagnosis of the tropical Atlantic near-equatorial SST bias in a directly coupled atmosphere-ocean general circulation model. Geophys Res Lett 32:L01703. doi:10.1029/2004GL021707

DiNezio PN, Kirtman BP, Clement AC, Lee S-K, Vecchi GA, Wittenberg AT (2012) Mean climate controls on the simulated response of ENSO to increasing greenhouse gases. J Clim 25:7399-7420. doi:http://dx.doi.org/10.1175/JCLI-D-11-00494.1

Enfield DB, Mestas-Nuñez AM, Trimble PJ (2001) The Atlantic multidecadal oscillation and its relation to rainfall and river flows in the continental US. Geophys Res Lett 28:2077-2080

Gent PR, Yeager SG, Neale RB, Levis S, Bailey DA (2010) Improvements in a half degree atmosphere/land version of the CCSM. Clim Dyn 34:819-833

Gent PR, and coauthors (2011) The community climate system model version 4. J Clim 24:4973-4991

Giannini A, Saravanan R, Chang P (2003) Oceanic forcing of Sahel rainfall on interannual to interdecadal time scales. Science 302:1027-1030

Goes M, Wainer I (2003) Equatorial currents transport changes for extreme warm and cold events in the Atlantic Ocean. Geophys Res Lett 30:8006. doi:10.1029/2002GL015707

Goldenberg SB, Landsea CW, Mestas-Nuñez AM, Gray WM (2001) The recent increase in Atlantic hurricane activity: Causes and implications. Science 293:474-479

Good SA, Martin MJ, Rayner NA (2013) EN4: quality controlled ocean temperature and salinity profiles and monthly objective analyses with uncertainty estimates. J Geophys Res 118: 6704-6716. doi:10.1002/2013JC009067

Grodsky SA, Carton JA, Nigam S, Okumura YM (2012) Tropical Atlantic biases in CCSM4. J Clim 25:3684-3701. doi: http://dx.doi.org/10.1175/JCLI-D-11-00315.1

Gu G, Adler RF (2004) Seasonal evolution and variability associated with the West African monsoon system. J Clim 17:3364-3377

Hazeleger W, Haarsma RJ (2005) Sensitivity of tropical Atlantic climate to mixing in a coupled ocean–atmosphere model. Clim Dyn 25:387-399

Hu Z-Z, Huang B, Pegion K (2008) Low cloud errors over the southeastern Atlantic in the NCEP CFS and their association with lower-tropospheric stability and air-sea interaction. J Geophys Res 113:D12114. doi:10.1029/2007JD009514

Hu Z-Z, Huang B, Hou Y-T, Wang W, Yang F, Stan C, Schneider EK (2011) Sensitivity of tropical climate to low-level clouds in the NCEP climate forecast system. Clim Dyn 36:1795-1811

Huang B, Hu Z-Z, Jha B (2007) Evolution of model systematic errors in the tropical Atlantic basin from coupled climate hindcasts. Clim Dyn 28:661-682

Hunke EC, Lipscomb WH (2008) CICE: The Los Alamos sea ice model user's manual, version 4. Los Alamos National Laboratory Tech Rep, LA-CC-06-012, 76pp

Hurrel JW, Hack JJ, Shea D, Caron JM, Rosinski J (2008) A new sea surface temperature and sea ice boundary dataset for the Community Atmosphere Model. J Clim 21:5145-5153

Kirtman BP, and coauthors (2012) Impact of ocean model resolution on CCSM climate simulations. Clim Dyn 39:1303-1328

Large WG, Danabasoglu G (2006) Attribution and impacts of upper-ocean biases in CCSM3. J Clim 19:2325–2346. doi: http://dx.doi.org/10.1175/JCLI3740.1

Large WG, Yeager SG (2004) Diurnal to decadal global forcing for ocean and sea ice models: the data sets and climatologies. NCAR Tech. Note 460+STR, 105 pp

Large WG, Yeager SG (2008) The global climatology of an interannually varying air–sea flux data set. Clim Dyn 33:341-364. doi:10.1007/s00382-008-0441-3

Lawrence DM, and coauthors (2011) Parameterization improvements and functional and structural advances in version 4 of the Community Land Model. J Adv Model Earth Syst 3:M03001. doi:10.1029/2011MS000045

Lee S-K, Csanady GT (1999a) Warm water formation and escape in the upper tropical Atlantic Ocean: 1. A literature review. J Geophys Res 104:29561-29571. doi:10.1029/1999JC900079.

Lee S-K, Csanady GT (1999b) Warm water formation and escape in the upper tropical Atlantic Ocean: 2. A numerical model study. J Geophys Res 104:29573–29590. doi:10.1029/1999JC900078.

Lee S-K, Enfield DB, Wang C (2007) What drives the seasonal onset and decay of the Western Hemisphere warm pool? J Clim 20:2133-2146

Lee S-K, Wang C (2008) Tropical Atlantic decadal oscillation and its potential impact on the equatorial atmosphere–ocean dynamics: A simple model study. J Phys Oceanogr 38:193–212. doi: http://dx.doi.org/10.1175/2007JPO3450.1

Lee S-K, Enfield DB, Wang C (2011) Future impact of differential inter-basin ocean warming on Atlantic hurricanes. J Clim 24:1264-1275

Liu H, Wang C, Lee S-K, Enfield DB (2013) Atlantic warm pool variability in the CMIP5 simulations. J Clim 26:5315-5336. doi: 10.1175/JCLI-D-12-00556.1

Liu Y, Lee S-K, Muhling BA, Lamkin JT, Enfield DB (2012) Significant reduction of the Loop Current in the 21st century and its impact on the Gulf of Mexico. J Geophys Res 117: C05039. doi:10.1029/2011JC007555

Manabe S, Bryan K (1969) Climate calculations with a combined ocean-atmosphere model. J Atmos Sci 26:786-789

Meehl G, Covey C, McAvaney B, Latif M, Stouffer R (2005) Overview of the coupled model intercomparison project (CMIP). Bull Amer Meteor Soc 86:89-93

Mechoso CR, and coauthors (1995) The seasonal cycle over the tropical Pacific in coupled ocean–atmosphere general circulation models. Mon Wea Rev 123:2825-2838

Neale RB, and coauthors (2010) Description of the NCAR Community Atmosphere Model (CAM4.0). NCAR Tech Note 485+STR, 212 pp.

Okumura Y, Xie S-P (2004) Interaction of the Atlantic equatorial cold tongue and the African monsoon. J Clim 17:3589–3602

Patricola CM, Chang P, Saravana R, Li M, Hsieh J-S (2011) An investigation of the tropical Atlantic bias problem using a high-resolution coupled regional climate model. US CLIVAR Variations 9 U.S. CLIVAR Office Washington DC 9-12. [Available online at http://www.usclivar.org/Newsletter/V9N2.pdf.]

Rienecker MM et al (2011) MERRA: NASA's Modern-Era Retrospective Analysis for Research and Applications. J Clim 24:3624-3648. doi:10.1175/JCLI-D-11-00015.1

Richter I, Xie S-P (2008) On the origin of equatorial Atlantic biases in coupled general circulation models. Clim Dyn 31:587-598

Richter I, Xie S-P, Wittenberg AT, Masumoto Y (2012) Tropical Atlantic biases and their relation to surface wind stress and terrestrial precipitation. Clim Dyn 38:985–1001

Saha S, and coauthors (2006) The NCEP climate forecast system. J Clim 19:3483–3517. doi: http://dx.doi.org/10.1175/JCLI3812.1

Seo H, Jochum M, Murtugudde R, Miller AJ (2006) Effect of ocean mesoscale variability on the mean state of tropical Atlantic climate. Geophys Res Lett 33:L09606. doi:10.1029/2005GL025651

Toniazzo T, Woolnough S (2013) Development of warm SST errors in the southern tropical Atlantic in CMIP5 decadal hindcasts. Clim Dyn doi:10.1007/s00382-013-1691-2

Wahl S, Latif M, Park W, Keenlyside N (2011) On the tropical Atlantic SST warm bias in the Kiel climate model. Clim Dyn 36:891-906

Wang C, Enfield DB, Lee S-K, Landsea CW (2006) Influences of the Atlantic warm pool on Western Hemisphere summer rainfall and Atlantic hurricanes. J Clim 19:3011–3028. doi: http://dx.doi.org/10.1175/JCLI3770.1

Wang C, Lee S-K (2007) Atlantic warm pool, Caribbean low-level jet, and their potential impact on Atlantic hurricanes. Geophys Res Lett 34:L02703. doi:10.1029/2006GL028579

Webster PJ, Holland GJ, Curry JA, Chang H-R (2005) Changes in tropical cyclone number, duration, and intensity in a warming environment. Science 309:1844-1846

Williams KD, and coauthors (2013) The Transpose-AMIP II experiment and its application to the understanding of southern ocean cloud biases in climate models. J Clim, 26:3258–3274. doi: http://dx.doi.org/10.1175/JCLI-D-12-00429.1

Vizy EK, Cook KH (2001) Mechanisms by which Gulf of Guinea and eastern North Atlantic sea surface temperature anomalies can influence African rainfall. J Clim 14:795–821

Voldoire A, Claudon M, Caniaux G, Giordani H, Roehrig R (2014) Are atmospheric biases responsible for the tropical Atlantic SST biases in the CNRM-CM5 coupled model? Clim Dyn doi:10.1007/s00382-013-2036-x

Xie S-P, Carton JA (2004) Tropical Atlantic variability: Patterns, mechanisms, and impacts, in Earth's Climate: The Ocean-Atmosphere Interaction. Geophys Monogr Ser vol. 147, edited by Wang C, Xie S-P, Carton JA, pp. 121–142, AGU Washington D.C. doi:10.1029/147GM07

Xie S-P, Deser C, Vecchi GA, Ma J, Teng H, Wittenberg AT (2010) Global warming pattern formation: Sea surface temperature and rainfall. J Clim 23:966–986.

Xu Z, Chang P, Richter I, Kim W, Tang G (2014) Diagnosing southeast tropical Atlantic SST and ocean circulation biases in the CMIP5 ensemble. Clim Dyn doi:10.1007/s00382-014-2247-9

Yu JY, Mechoso CR (1999) Links between annual variations of Peruvian stratocumulus clouds and of SST in the eastern equatorial Pacific. J Clim 12:3305-3318

Figure captions

Figure 1. Annually averaged climatological SSTs in the tropical Atlantic from (a) EN4, a global quality controlled ocean temperature data set provided by the Met Office Hadley Centre (Good et al. 2013), for 1949-2005, and (b) CCSM4 historical simulation for 1949-2005. The SST bias in CCSM4 is shown in (c). The unit is °C. The SST bias values higher than 6^{o}C are masked.

Figure 2. Annually averaged implicit SST bias in EXP_ATM due to (a) the net surface heat flux bias, which is computed by integrating the net heat flux bias in EXP_ATM for one year from January 1 to December 31, then dividing it by 12 months. Contributions by (b) shortwave radiative heat flux bias, (c) latent heat flux bias and (d) longwave radiative heat flux bias. The vectors in (c) show the annually averaged surface wind stress bias. The unit for the implicit SST bias is °C.

Figure 3. Annually averaged SST bias in EXP_OCN. The unit is °C.

Figure 4. Annually averaged implicit SST bias in (a) EXP_OCN and (b) EXP_ATM + EXP_OCN. (c) Annually averaged SST bias in EXP_CPL during the first year. The unit is °C. The implicit SST bias values higher than 12^{o}C are masked.

Figure 5. Time evolution of the SST bias in EXP_CPL during the first and second year. The unit is °C.

Figure 6. (1st column) Time evolution of the SST bias tendency in EXP_CPL during the first year. Time evolution of the implicit SST bias tendency in (2nd column) EXP_ATM + EXP_OCN, (3rd column) EXP_ATM, and (4th column) EXP_OCN. The unit is °C month^{-1}.

Figure 7. Time-longitude evolutions of (a) the SST bias tendencies along the equatorial Atlantic, and the contributions by (b) the surface heat flux errors and (c) errors involving ocean dynamic processes in EXP_CPL during the first year. Time-longitude evolutions of implicit SST bias tendencies in (d) EXP_ATM + EXP_OCN, (e) EXP_ATM and (f) EXP_OCN. The unit is °C month^{-1}.

Figure 8. Time-depth evolutions of the equatorial Atlantic temperature bias (shaded) and mixed layer depth (green solid line) averaged for 5ºS-5ºN obtained from EXP_OCN. The green dashed line is the mixed layer depth obtained from EN4.

Figure 9. Annually averaged implicit SST bias in (a,d,g) EXP_ATM, (b,e,h) EXP_OCN, and (c,f,i) EXP_ATM + EXP_OCN referenced to (a,b,c) COREv2, (d,e,f) ERA_INT, and (g,h,i) MERRA. The unit is °C. The SST bias values higher than 12°C are masked.

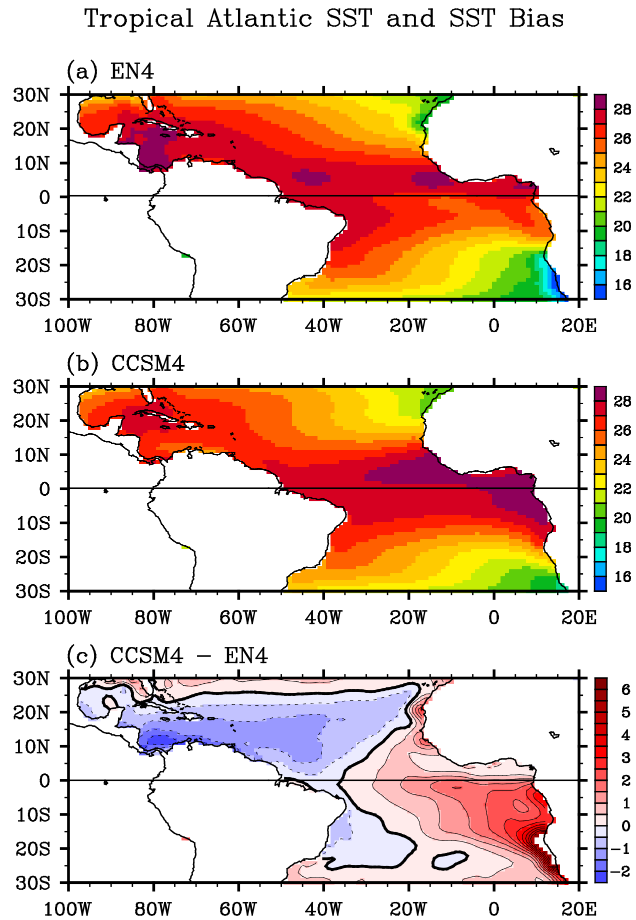

Figure 1. Annually averaged climatological SSTs in the tropical Atlantic from (a) EN4, a global quality controlled ocean temperature data set provided by the Met Office Hadley Centre (Good et al. 2013), for 1949-2005, and (b) CCSM4 historical simulation for 1949-2005. The SST bias in CCSM4 is shown in (c). The unit is °C. The SST bias values higher than 6^{o}C are masked.

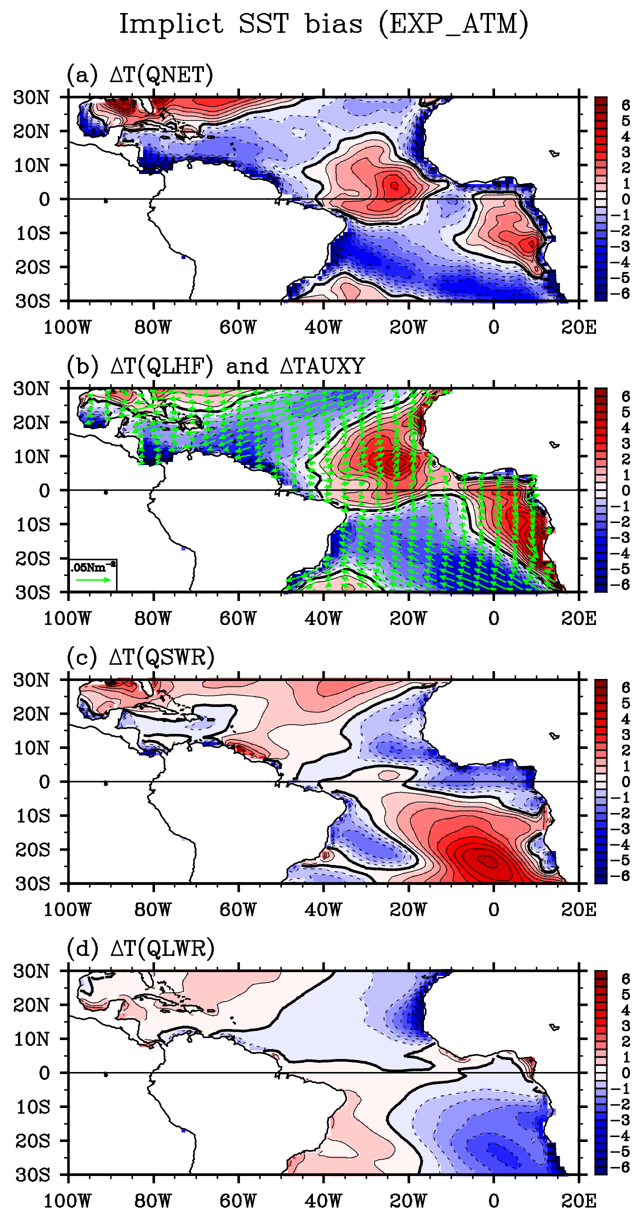

Figure 2. Annually averaged implicit SST bias in EXP_ATM due to (a) the net surface heat flux bias, which is computed by integrating the net heat flux bias in EXP_ATM for one year from January 1 to December 31, then dividing it by 12 months. Contributions by (b) shortwave radiative heat flux bias, (c) latent heat flux bias and (d) longwave radiative heat flux bias. The vectors in (c) show the annually averaged surface wind stress bias. The unit for the implicit SST bias is °C.

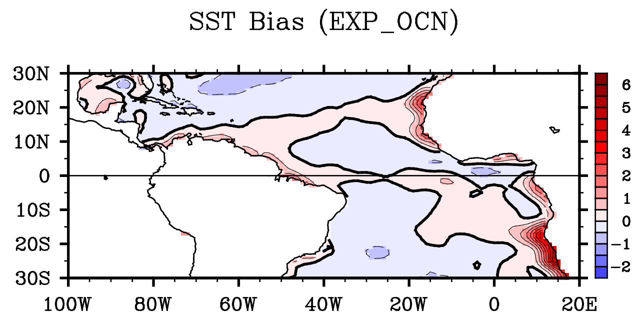

Figure 3. Annually averaged SST bias in EXP_OCN. The unit is °C.

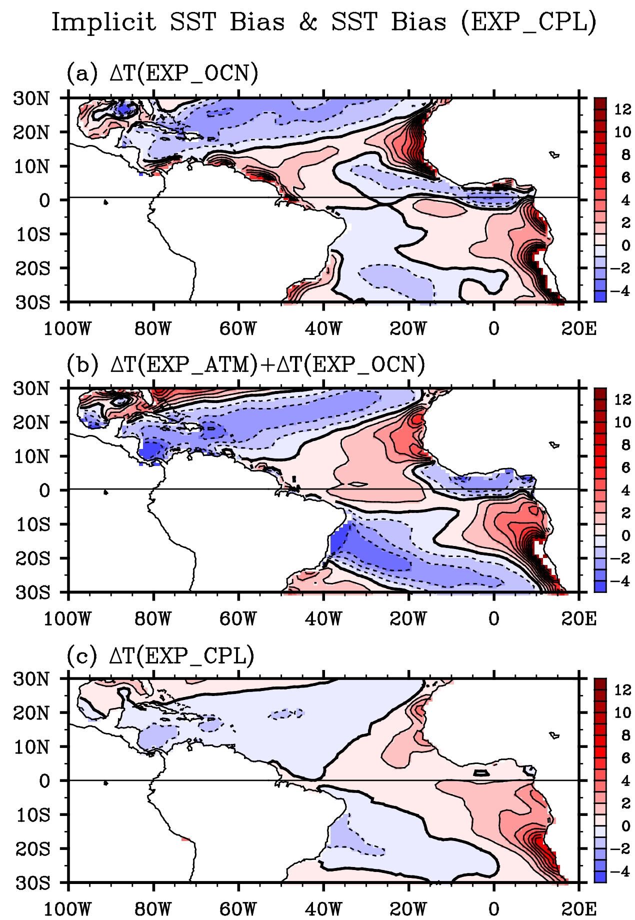

Figure 4. Annually averaged implicit SST bias in (a) EXP_OCN and (b) EXP_ATM + EXP_OCN. (c) Annually averaged SST bias in EXP_CPL during the first year. The unit is °C. The implicit SST bias values higher than 12°C are masked.

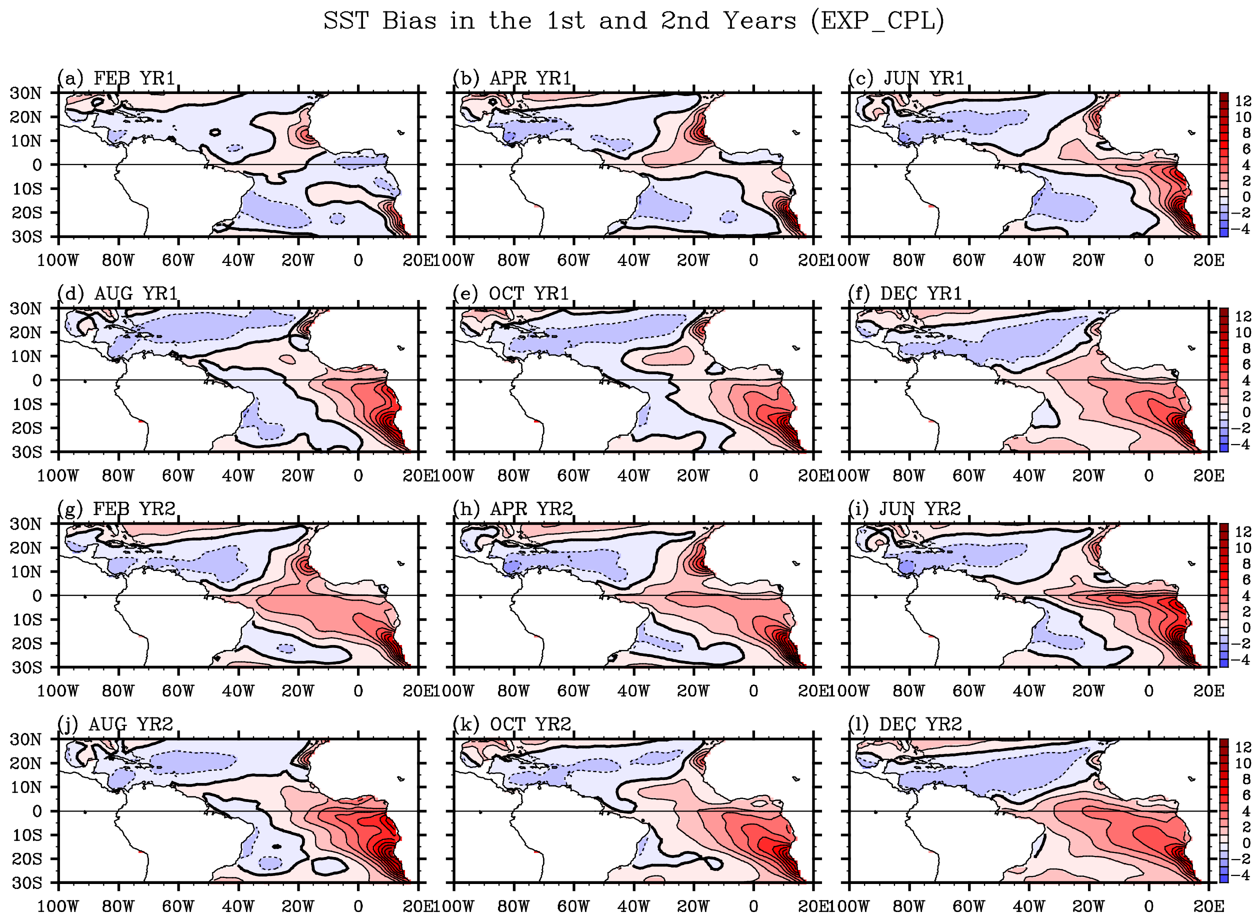

Figure 5. Time evolution of the SST bias in EXP_CPL during the first and second year. The unit is °C.

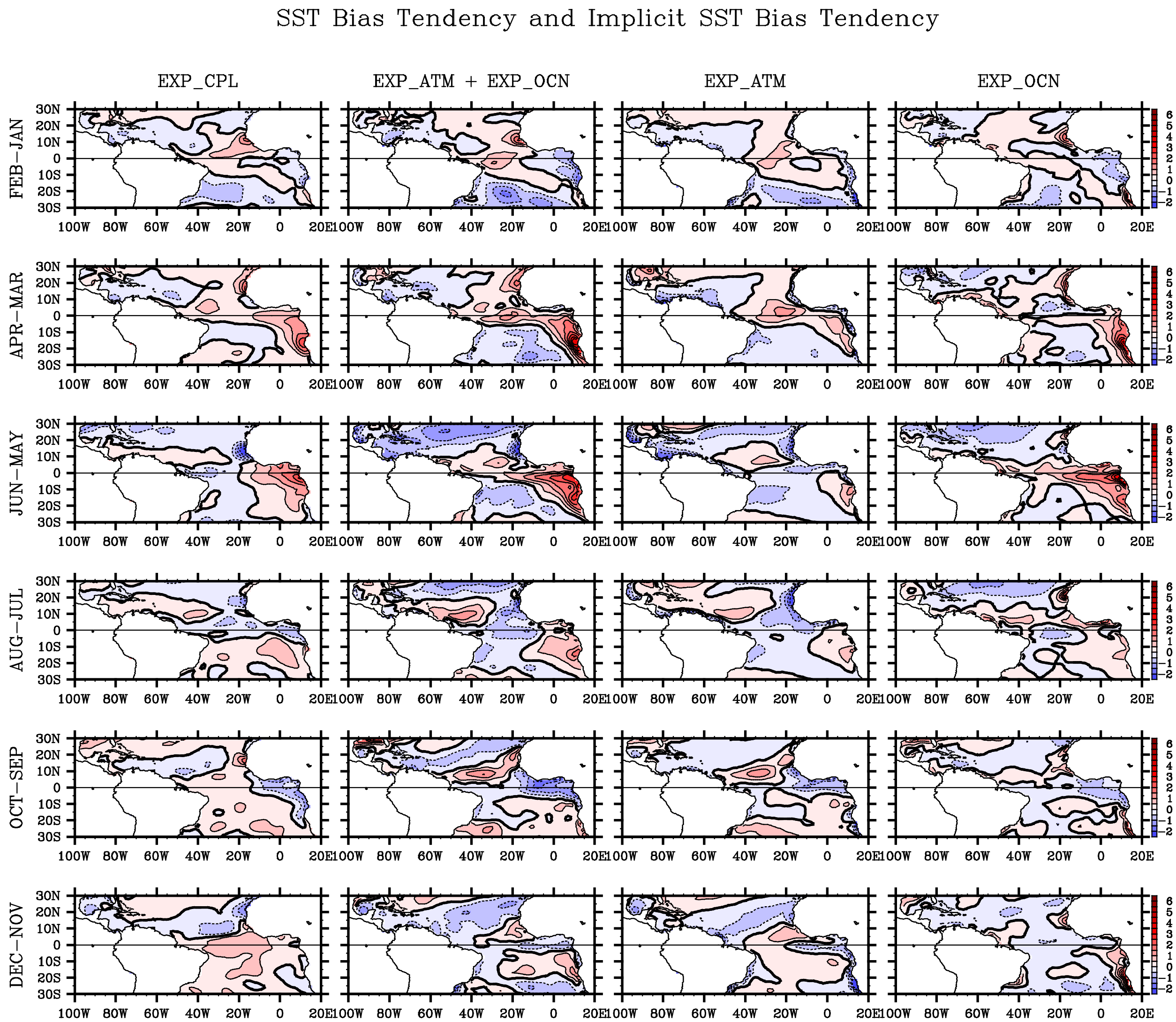

Figure 6. (1st column) Time evolution of the SST bias tendency in EXP_CPL during the first year. Time evolution of the implicit SST bias tendency in (2nd column) EXP_ATM + EXP_OCN, (3rd column) EXP_ATM, and (4th column) EXP_OCN. The unit is °C month^{-1}.

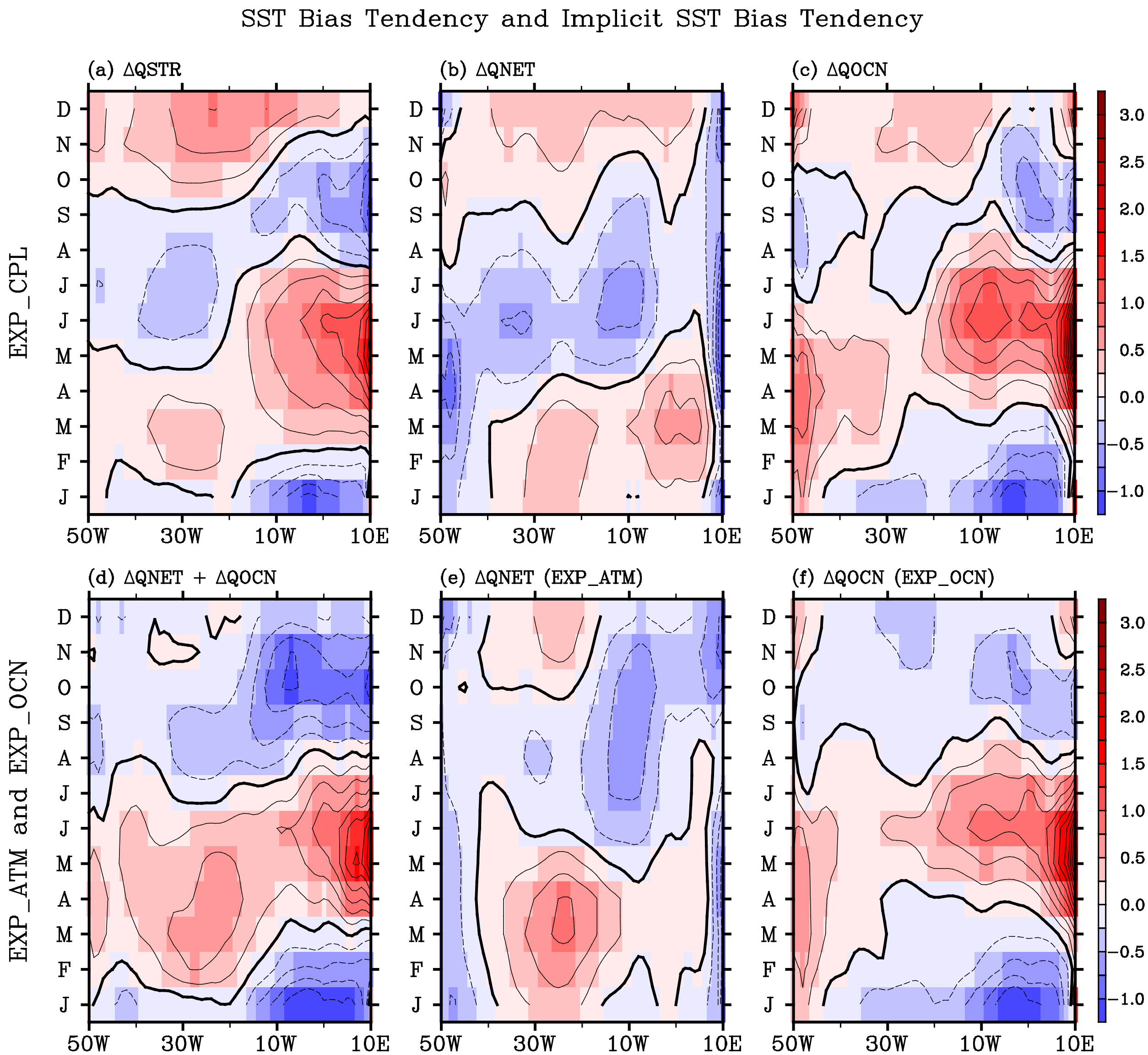

Figure 7. Time-longitude evolutions of (a) the SST bias tendencies along the equatorial Atlantic, and the contributions by (b) the surface heat flux errors and (c) errors involving ocean dynamic processes in EXP_CPL during the first year. Time-longitude evolutions of implicit SST bias tendencies in (d) EXP_ATM + EXP_OCN, (e) EXP_ATM and (f) EXP_OCN. The unit is °C month^{-1}.

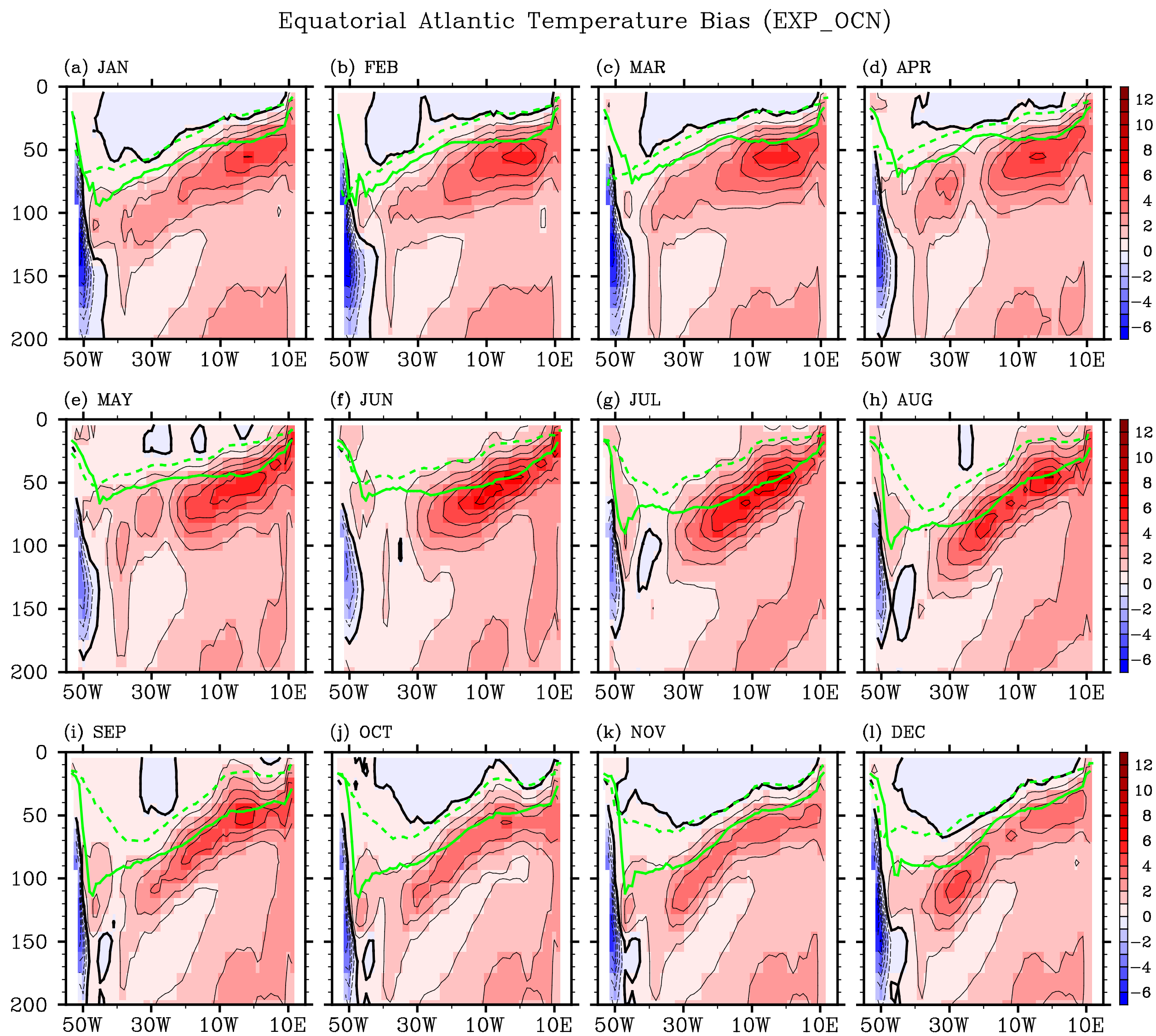

Figure 8. Time-depth evolutions of the equatorial Atlantic temperature bias (shaded) and mixed layer depth (green solid line) averaged for 5ºS-5ºN obtained from EXP_OCN. The green dashed line is the mixed layer depth obtained from EN4.

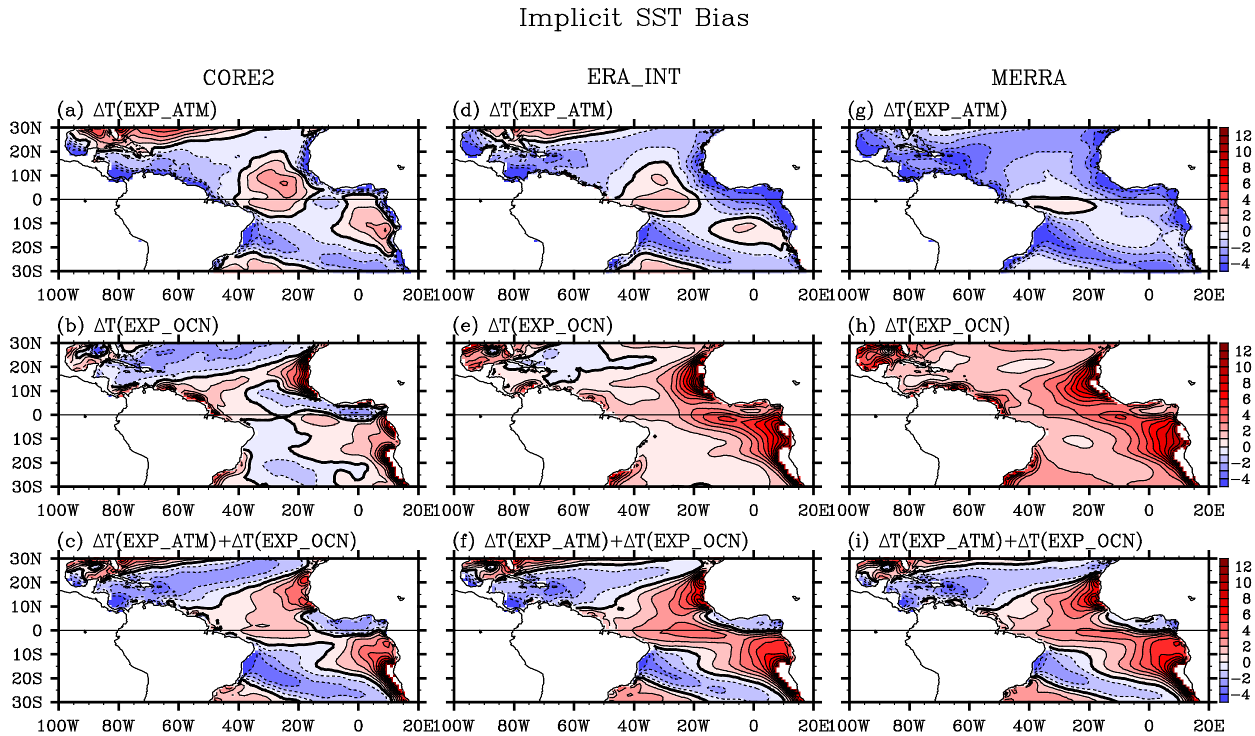

Figure 9. Annually averaged implicit SST bias in (a,d,g) EXP_ATM, (b,e,h) EXP_OCN, and (c,f,i) EXP_ATM + EXP_OCN referenced to (a,b,c) COREv2, (d,e,f) ERA_INT, and (g,h,i) MERRA. The unit is °C. The SST bias values higher than 12°C are masked.